Journal of Earth Science, Vol. 36, No. 4, p. 1867–1876, August 2025 *ISSN 1674-487X*
Printed in China
https://doi.org/10.1007/s12583-025-0196-3

Editorial

Characterization of Charged Lunar Dust in Multi-Source Irradiation Environments and Its Ground Simulation

Yun Chen[1], **Lifang Li**[*1, 2], **Jihong Yan**[*2], **Chengyue Sun**[2], **Yunlong Li**[2], **Dandan Ju**[2], **Chunlong Wang**[2]

1. *National Key Laboratory of Aerospace Mechanism*, *Harbin Institute of Technology*, *Harbin* 150001, *China*
2. *National Key Laboratory of Space Environment and Matter Behaviors*, *Harbin Institute of Technology*, *Harbin* 150001, *China*

0 INTRODUCTION

The lunar surface lacks an atmosphere and is continuously subjected to a combination of space weathering factors such as cosmic rays, solar wind, and micrometeorite impacts, forming a several-meter-thick lunar regolith (Sorokin et al., 2020). Among these factors, multi-source irradiation on the lunar surface, including ultraviolet (UV) rays, X-rays, and high-energy particle flux, has a strong influence on the formation and evolution of lunar surface materials. This not only alters the physical, chemical, mineralogical, and spectral properties of lunar materials but also leads to complex charge accumulation on the surface of lunar soil particles, causing the migration of charged lunar dust. The charging behavior of lunar dust is closely related to the properties of lunar dust particles, including size, morphology, surface composition, and electromagnetic properties (Gan et al., 2025; Jin et al., 2024). Dust migration is influenced by the surrounding space environment, including irradiation intensity, lunar surface temperature, and topography, as well as the resulting electric fields that drive particle movement. On the sunlit side of the Moon, which is affected by the solar wind, the potential is approximately 3 to 10 V (Stubbs et al., 2014), while the shadowed side of the Moon is within the lunar plasma tail, where the potential can reach as low as -1 000 V. At the lunar terminator, the contrasting electric potentials can create dust-related phenomena, such as lunar horizon glow and dust fountains, particularly under low gravity conditions (Criswell, 1973). These migrating charged dust particles could challenge future lunar exploration missions by impacting equipment performance. For example, they may reduce the efficiency of solar panels and compromise the cleanliness of instrument surfaces.

Additionally, dust migration caused by lunar exploration, such as engine plumes and lunar rover movement, can lead to triboelectric charging and irradiation-induced charging of lunar dust particles under high-energy irradiation and extreme temperature conditions (Wang et al., 2022). These charged particles impact the lunar surface environment and the normal functioning of equipment. Engine plumes or rover movement can suspend lunar dust, causing it to enter localized electric fields. Under these conditions, the charged dust particles may migrate along specific directions due to electrostatic forces, resulting in secondary contamination or interference. This can degrade or even disable key systems such as radiators and optical devices, causing mechanical components to seize. Charged dust can threaten lunar dust sampling and *in-situ* measurements, creating substantial risks for lunar exploration missions (Zhang et al., 2024). The Apollo 11 mission was the first to evaluate the impact of plume-induced dust (Morris et al., 2011). During the Apollo 15 mission, plume-induced dust hindered camera imaging and obstructed the safe landing of the spacecraft, which eventually landed on a slope with an inclination of up to 11° (Immer et al., 2011).

Lunar exploration and *in-situ* resource utilization (ISRU) are emerging, but lunar dust hazards are becoming a critical concern. In 2017, NASA launched the “Artemis” program to establish a lunar base near the Moon’s south pole. This base is designed to support the safe Earth-Moon commutes of astronauts and facilitate the *in-situ* utilization of resources such as water ice, serving as a technological foundation for future manned Mars missions (Smith et al., 2020). Similarly, the European Space Agency (ESA) has proposed various extraterrestrial exploration projects, including the “Moon Village” concept (Woerner and Foing, 2016). This initiative envisions a permanent settlement at the rim of Shackleton Crater near the lunar south pole, where large-scale resource development and scientific research will be conducted. China Lunar Exploration Project will conduct scientific investigations in the permanently shadowed regions of the lunar south pole. By 2035, China plans to complete the construction of a basic model of the International Lunar Research Station (ILRS). The station will be capable of long-term autonomous operation and will support short-

*Corresponding authors: lilifang@hit.edu.cn; jhyan@hit.edu.cn

Manuscript received March 10, 2025.
Manuscript accepted April 27, 2025.

Chen Yun, Li Lifang, Yan Jihong, Sun Chengyue, Li Yunlong, Ju Dandan, Wang Chunlong, 2025. Characterization of Charged Lunar Dust in Multi-Source Irradiation Environments and Its Ground Simulation. *Journal of Earth Science*, 36(4): 1867–1876. https://doi.org/10.1007/s12583-025-0196-3. http://en.earth-science.net

term human habitation with scalability and maintainability (Zhou et al., 2024). As lunar activities expand, assessing the adhesive effects of charged dust on spacecraft is increasingly critical. Unlike the short-term surface visits of the Luna and Apollo programs, future missions focus on long-term habitation, human presence, and resource utilization. These efforts require careful consideration of spacecraft reliability, surface infrastructure durability, and overall operational safety in the lunar environment.

Therefore, the lunar surface environment serves as an ideal testing ground for the formation and evolution of lunar materials and space exploration activities. However, the Moon's extreme environmental conditions pose numerous challenges, especially low gravity, high vacuum, large temperature variations, micrometeorite impacts, charged lunar dust, and multi-source irradiation. These challenges include spacecraft material degradation, electrical charging and discharging, and impact damage. Electrostatic adhesion further complicates operations, posing risks to the safety and reliability of spacecraft and lunar infrastructure. To address these challenges, ground-based simulations are crucial for assessing the hazards of charged lunar dust on surface exploration. This requires investigating fundamental processes, including dust charging mechanisms. Advancing large-scale lunar environment simulation facilities is essential to support these studies and enhance our understanding of dust-related risks (Wang et al., 2024).

1 LUNAR SURFACE ENVIRONMENTAL SIMULATION FACILITIES

The lunar environment is complicated, exposing lunar-based equipment to various failure modes throughout its operational lifespan. This complexity makes it challenging to accurately predict performance degradation. Ground-based simulations are essential for studying lunar surface effects and electrical charging failures. Research should focus on charge dynamics under multi-source irradiation, including UV, X-rays, and electron beams. UV and X-ray radiation continuously affect the lunar surface environment, primarily originating from solar flares and cosmic rays. Electron beams play a crucial role in transporting lunar surface dust, especially within the electron cloud region during magnetotail crossings and in the plasma wake (Gan et al., 2025; Denevi et al., 2023). Therefore, existing lunar environment simulation facilities primarily evaluate the impact of charged lunar dust on functional surfaces, mechanical components, and astronaut activities. Key concerns include contamination of optical devices, mechanical obstruction of moving parts, and reduced sealing performance of spacesuits (Wei, 2022). As a result, the development of simulation technologies for the multi-source irradiation charging environment on the lunar surface should be prioritized. This involves constructing multi-factor coupled lunar environment simulation systems to ensure the long-term reliable operation of lunar-based equipment during their service period. Currently, the large-scale devices capable of simulating the charged dust induced by lunar surface irradiation include the following equipment.

(1) Lunar dust adhesion bell jar (LDAB) at NASA Glenn Research Center (Gaier et al., 2010)

LDAB (Figure 1a) is used to simulate the lunar dust environment and its effects. It is a vacuum chamber capable of testing material samples less than about 7 cm in diameter, with a vacuum level of 10^{-6} Pa. The chamber can simulate thermal cycles, disperse dust, and use radio frequency hydrogen/helium plasma to mimic the solar wind. It is equipped with an *in-situ* xenon arc lamp solar simulator to enable *in-situ* solar irradiation simulations. A microscopic imaging system is integrated to observe the deposition characteristics of dust particles on the sample surface. Additionally, a quartz crystal microbalance is employed for precise measurement of dust deposition mass. A mass spectrometer is also installed to monitor and record real-time changes in the composition of residual gases within the chamber.

(2) Lunar environment test system (LETS) at Marshall Space Flight Center (Craven et al., 2009)

LETS (Figure 1b) is designed to simulate typical lunar surface environments. It utilizes a vacuum system equipped with a low-temperature pump, achieving a vacuum level of up to 10^{-5} Pa. The LETS horizontal chamber has a diameter of 0.8 m and a length of 1.2 m, with a liquid nitrogen heat sink and a quartz lamp heating array that allows for temperature control within a range of -190 to +150 °C. The system is equipped with three irradiation sources, including a vacuum ultraviolet lamp, an electron gun, and a low-energy proton source. A distinctive feature of LETS is its large lunar surface simulation bed (approximately 45 cm × 105 cm × 15 cm), which can hold up to 75 kg of lunar soil simulant. This setup enables experiments to study the charging, suspension, and movement of dust particles, as well as the simulation of lunar surface irradiation conditions.

(3) The Mars simulation chamber (MSC) at the Kennedy Space Center (Hintze et al., 2010)

The device features a stainless steel vacuum chamber structure, equipped with a high-precision vacuum pump system and pressure control unit (Figure 1c). An atmospheric composition simulation module is integrated within the chamber, along with a fused quartz observation window that enables multi-wavelength (UV-visible-infrared) optical observation. The effective experimental space inside the chamber measures 50 cm in diameter and 70 cm in length. A 1 000 W xenon arc lamp serves as the ultraviolet irradiation source. This facility provides a broad temperature control range from -100 to +160 °C and accurately simulates surface atmospheric conditions, including temperature, pressure, and gas composition of target celestial bodies. It also reproduces solar and ultraviolet irradiation characteristics while simulating the scattering and attenuation effects of atmospheric dust on incident light. The device applies to simulate the surface environment of celestial bodies such as the Moon, Mars, asteroids, and comets. It also supports planetary upper-

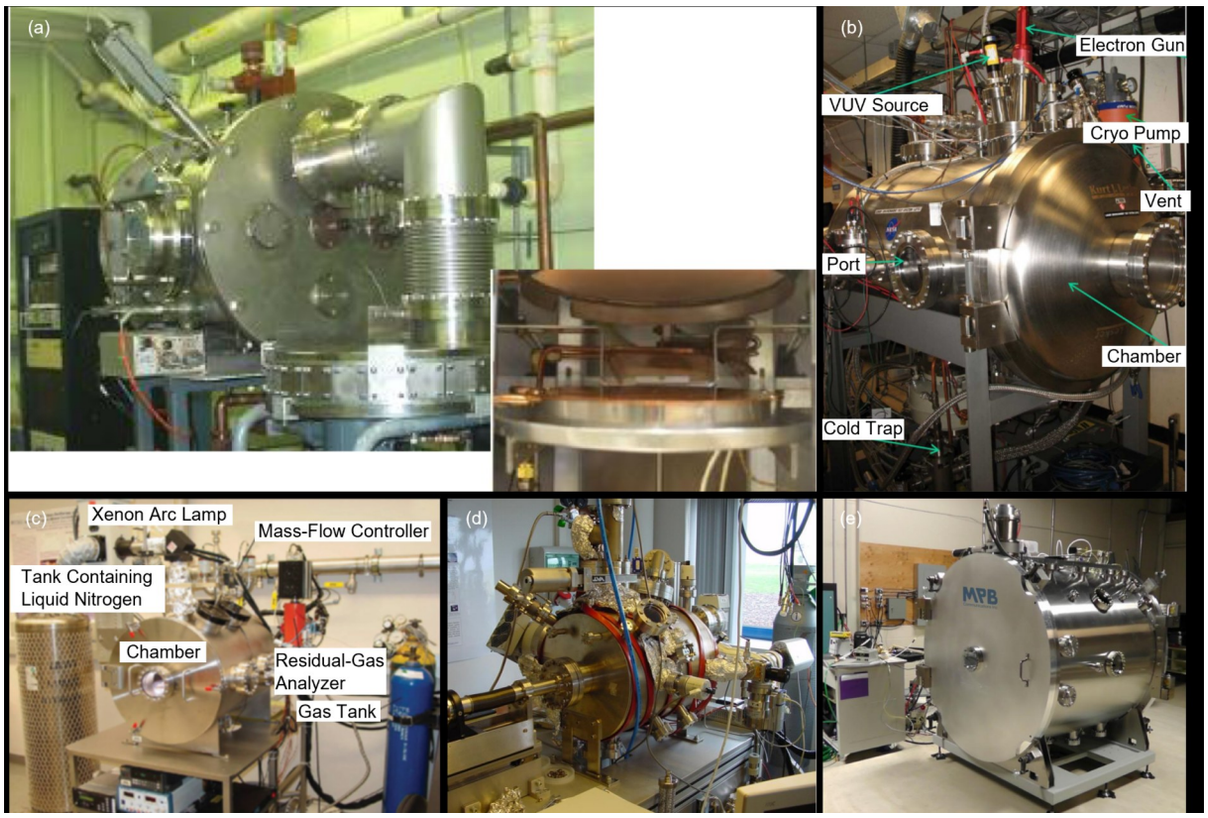

Figure 1. Large-scale lunar environmental simulation systems. (a) Lunar dust adhesion bell jar (LDAB); (b) lunar environment test system (LETS); (c) the Mars simulation chamber (MSC); (d) planetary atmosphere and surfaces chamber (PASC); (e) dusty thermo-vacuum planetary environment simulator (DTVAC).

atmosphere reconstruction and can simulate atmospheric environments up to 100 km altitude on Earth.

(4) Planetary atmosphere and surfaces chamber (PASC) at the Spanish National Institute for Aerospace Technology (Mateo-Marti, 2014)

PASC (Figure 1d) is a multifunctional simulation facility for planetary environments, capable of generating computer-controlled gas compositions, atmospheric pressure, and sample temperatures. The test space is an ultra-high vacuum chamber with a diameter of 40 cm and a length of 50 cm, achieving an ultimate vacuum level of up to 5×10^{-7} Pa. It is equipped with a 5 keV electron irradiation source, a 5 keV ion irradiation source, and a deuterium lamp UV irradiation source with a wavelength range of 200 to 500 nm. The temperature of the sample can be regulated from −269 to 52 °C by a commercial helium cooling system connected to the sample holder. Sample size ranges are from 5 to 35 mm in diameter.

(5) Dusty thermo-vacuum planetary environment simulator (DTVAC) at the University of Winnipeg, Canada (Roman et al., 2017)

DTVAC (Figure 1e) is used to validate the reliability of detector subcomponents and instruments under simulated lunar or Martian surface conditions. It combines controlled vacuum, simulated solar irradiation, and temperature regulation. The system is equipped with a large-area planetary dust simulant dispenser and a triboelectric charger. The chamber allows temperature control within the range of 80 to 393 K. Dust charging can be achieved through various methods, including 193 nm UV laser excitation, UV LED annular illumination, parallel and saddle-shaped electrostatic fields, field-assisted UV charging, and electrical contact charging. The chamber has an unladen vacuum level of 10^{-5} Pa and can reach a laden vacuum level of up to 10^{-2} Pa. The dust dispersion area is 1.1 m × 1.1 m, with a dispersing rate ranging from 0.001 to 0.35 g/(cm²·h). The DTVAC successfully simulates and controls lunar surface environmental factors such as temperature extremes, charged dust, UV irradiation, and vacuum conditions.

The five devices mentioned above can simulate the lunar surface environment with charged dust, with a maximum chamber size of less than 3 m in each case. All of these devices utilize ultraviolet (UV) irradiation sources. Among them, NASA's lunar environment test system (LETS) incorporates UV, electron, and proton irradiation. However, none of the systems are equipped with X-ray irradiation sources. Furthermore, none of the devices provides a comprehensive irradiation system that combines UV, X-ray, and electron irradiation, the three typical sources of surface irradiation on the Moon.

2 LUNAR DUST CHAMBER AT HARBIN INSTITUTE OF TECHNOLOGY

Harbin Institute of Technology, supported by the National Major Scientific and Technological Infrastructure

Table 1 Technical parameters of large-scale lunar environmental simulation systems

Equipment Name	Simulated environment	Key technical indicators	Research objects and functions
NASA: lunar dust adhesion bell jar (LDAB)	Simulation of lunar dust environment and corresponding effects	Size: Φ 1.8 m × 2.4 m (Φ denotes diameter) Vacuum: 10^{-6} Pa Hydrogen/helium plasma source, xenon lamp	Lunar dust environment simulation, research on lunar regolith formation processes
NASA: lunar environment test system (LETS)	Lunar dust and irradiation environment	Size: Φ 0.8 m × 1.2 m Vacuum: 10^{-5} Pa UV, electron and proton irradiation	Charging, discharging, and migration behavior of dust particles and the lunar surface irradiation environment
NASA: The Mars simulation chamber (MSC)	Surface simulation for the Moon, Mars, asteroids, and comets	Simulated conditions: atmospheric temperature, pressure, composition, solar and UV irradiation Temperature: -100– +160 °C	Environmental response testing for various spacecraft and planetary exploration equipment
Spanish: Planetary atmosphere and surfaces chamber (PASC)	Multifunctional solar system planetary simulation	Vacuum: 5 × 10^{-7} Pa Electron source (5 keV), ion source (5 KeV), UV irradiation (200–500 nm)	Provides controlled atmospheric composition, large pressure range, and sample temperature environments
Canada: Dusty thermo-vacuum planetary environment simulator (DT-VAC)	Atmosphere-free solid and Mars surface simulation environments	Test Space: 1 m × 1 m × 0.9 m Vacuum: 10^{-5} Pa UV irradiation source and solar simulator	Planetary dust environment and load testing

Project, has successfully developed a world-leading multi-factor lunar environment simulation system known as the lunar dust chamber, as shown in Figure 2. This chamber precisely reproduces the coupling effects of various lunar surface environmental factors, including high vacuum, low temperature, ultraviolet irradiation, X-ray irradiation, electron irradiation, and micron-/submicron-sized charged dust particles. The primary purpose of this system is to facilitate fundamental research on the physical properties of charged lunar dust under multi-source irradiation and its effects on spacecraft systems. It focuses on the behavior of dust-plasma interactions and systematically investigates key physical processes, such as dust charging and discharging, levitation and sedimentation, migration, and dispersion. The system provides a crucial experimental platform and technical support for developing theoretical frameworks and evaluation methods related to the environmental effects on spacecraft performance in lunar dust conditions.

The system consists of a vacuum system, a cryogenic system, a lunar dust charging system, a lunar dust pretreatment and dispersion system, and an *in-situ* analysis system. The main chamber of the lunar dust chamber has a cylindrical section with an inner diameter of 4 m and a height of 5.5 m. The chamber achieves a high vacuum level of 10^{-6} Pa, and the thermal sink temperature is stably controlled below 100 K. The system is equipped with ultraviolet irradiation at 3.5 times the intensity of vacuum ultraviolet (VUV) irradiation constant (Figure 2c). The X-ray source operates within a voltage range of 30 to 80 kV (Figure 2d), while the electron irradiation energy ranges from 30 to 150 keV (Figure 2e). The dust dispersion system can uniformly disperse lunar dust particles ranging from 0.1 to 100 μm over a 1 m × 1 m area, with a dispersion uniformity exceeding 70%, which meets the technical requirements. Dispersion uniformity describes the homogeneity of the mass distribution of particles (lunar dust simulants). The rate of dust dispersing can be controlled from 0 to 40 g/cm^2. Additionally, the chamber integrates an *in-situ* analysis system, enabling real-time monitoring and analysis of both optical and electrical parameters.

2.1 Vacuum System

The vacuum system of the lunar dust chamber (Figure 3a) excels in its ability to prevent particle splashing and contamination under conditions of large-scale dust dispersion, simulating an extreme vacuum environment with micron- and nanoscale lunar dust. The system's pipeline interfaces are positioned at the top of the chamber, away from the dust dispersion area, and the system is composed of a clean, oil-free high-vacuum assembly (including cryopumps, turbomolecular pumps, and screw dry pumps) and an oil-free roughing system with Roots pumps and screw dry pumps. This configuration employs a multi-stage parallel vacuum pumping method.

The Roots and screw dry pumps create the initial vacuum, reducing the chamber pressure from atmospheric pressure to 10 Pa. Intelligent adjustable valves are included to control pumping speed and regulate the rate of pressure changes in stages. The pump inlets are equipped with vacuum filters capable of filtering out lunar dust simulants lifted by airflow disturbance larger than 3 μm to prevent dust contamination. The cryopump serves as the primary pumping system for achieving and maintaining experimental pressures. During cryopump precooling, a turbomolecular pump provides auxiliary evacuation, ensuring a smooth transition from the roughing vacuum to the optimal starting pressure for the cryopump. The system also enables leak detection within the chamber.

Under a thermal sink temperature of ⩽ 100 K, the system achieves the following design specifications: An unloaded ultimate pressure of ⩽ 1 × 10^{-4} Pa, with actual testing achieving 5.6 × 10^{-6} Pa; A loaded ultimate pressure of ⩽ 5 × 10^{-3} Pa with up to 30 kg of lunar dust simulants; A loaded ultimate pressure of ⩽ 5 × 10^{-1} Pa with up to 500 kg of lunar soil simulants. The system can operate

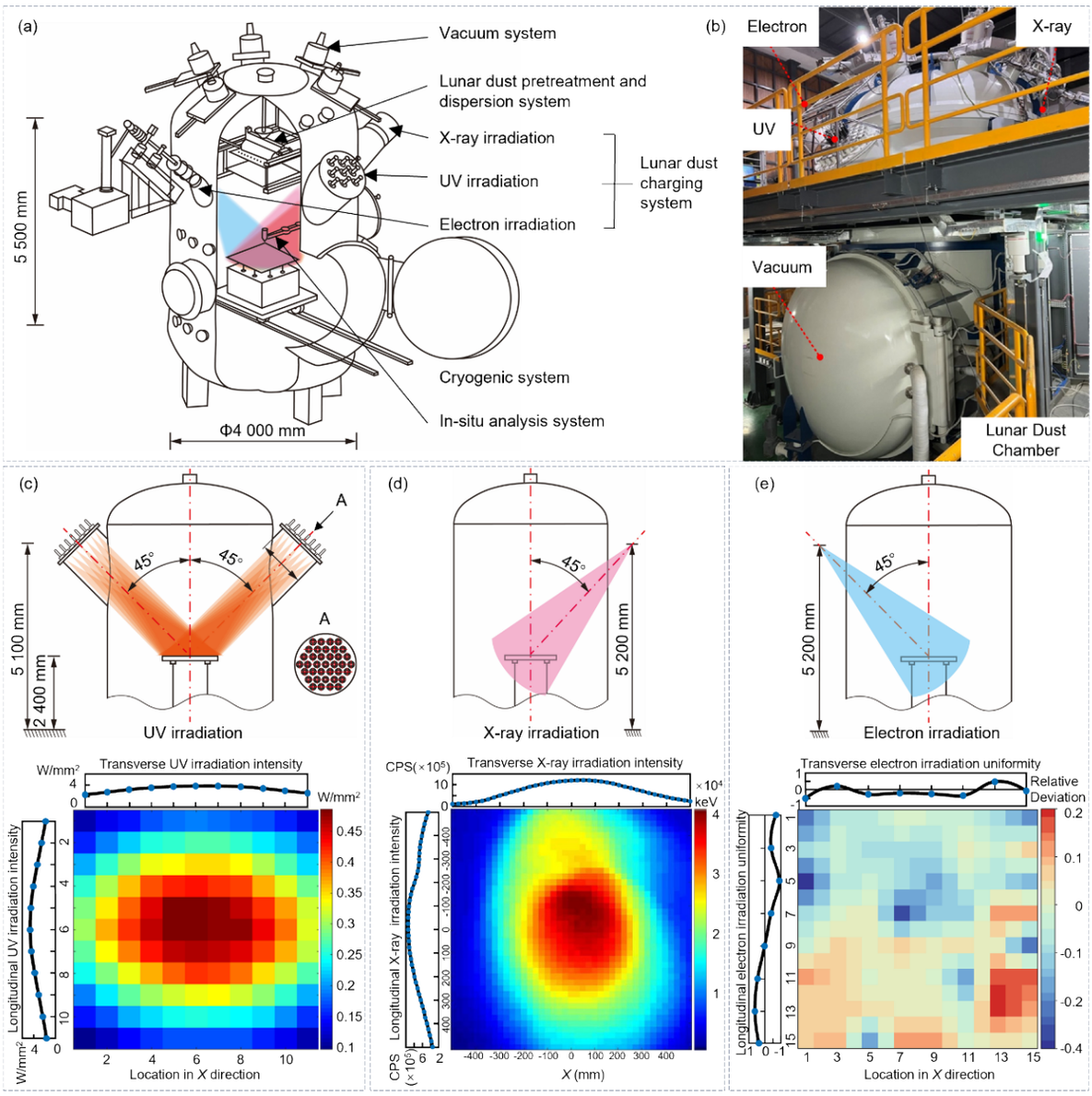

Figure 2. Overall layout of the lunar dust chamber at Harbin Institute of Technology. (a) Model of the lunar dust chamber shows the location of the core subsystems and the inner space. Φ denotes diameter and the unit is millimeters. (b) The lunar dust chamber. (c) UV irradiation source and the measured UV irradiation intensity distribution. A vacuum ultraviolet irradiation constant is equal to 0.1 W/mm^2. The integral of the irradiance intensity at each measuring point on the coordinate axis shows a Poisson distribution. (d) X-ray irradiation source and the measured irradiation intensity. The color changes from blue to red, indicating an increase in irradiation energy. The count rate (count per second) of the X-ray scintillation detector used in the test is marked as CPS. The intensity integral of each test point on the longitudinal and transverse axes also shows a Poisson distribution. (e) Electron irradiation source and the measured uniformity of the electron beam flux. The preset output energy of electron irradiation is 50 keV and the average energy measured (MeanT) is 54 keV. The relative deviation of the test results of each dose tablet to the average value ((T-MeanT)/MeanT) is shown in the heatmap. The accumulated relative deviation of each measuring point along the coordinate axis is shown in the curves on the left and above.

continuously for dust dispersion tests lasting ⩾ 30 h, maintaining a loaded ultimate pressure of ⩽ 5 × 10^{-3} Pa. The unloaded pressure of the chamber is close to the lunar vacuum environment (10^{-8} to 10^{-12} Pa). However, as the dust load increases, the degree of degassing from the dust piles also increases. This makes it increasingly difficult to maintain high vacuum conditions, as the rising gas pressure within the chamber reduces the achievable vacuum level.

The re-pressurization system adopts a nitrogen-air staged strategy to ensure reliability and adjustable re-pressurization rates. It incorporates a parallel structure with pneumatic baffle valves, adjustable butterfly valves, and manual valves. This design allows precise control of re-pressurization speed while ensuring manual operation in the event of system failure. Additionally, the system uses a diffuser design to effectively prevent direct airflow impact.

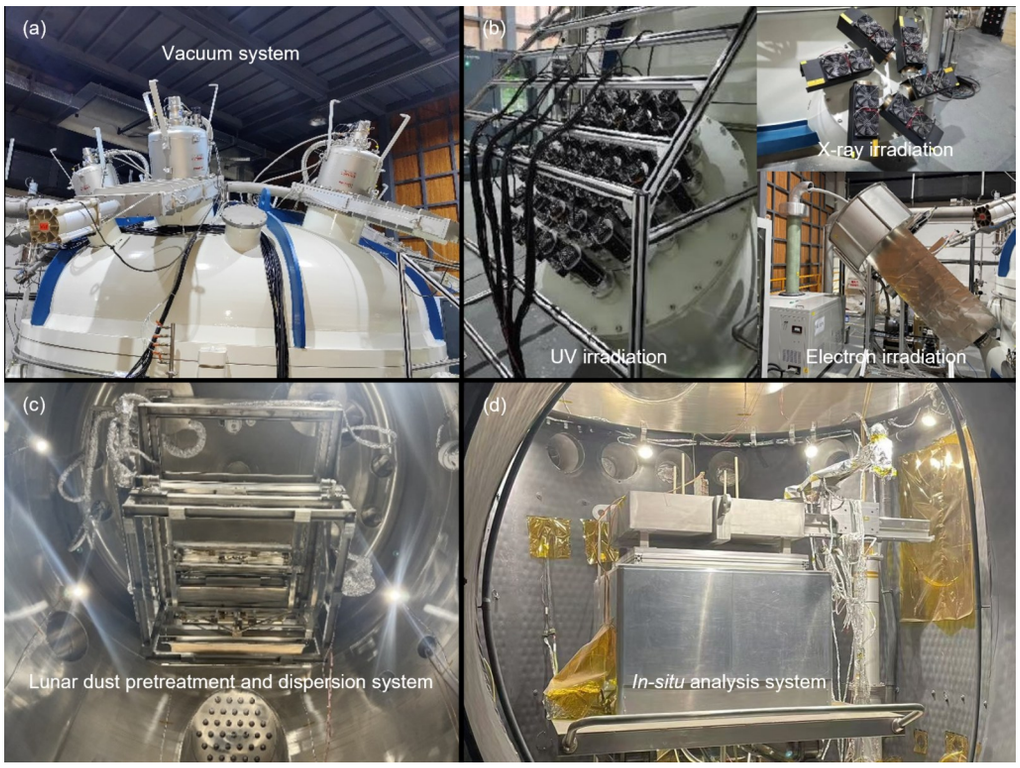

Figure 3. Core subsystems of the lunar dust chamber. (a) Vacuum system; (b) lunar dust charging system incorporating UV, X-ray, and electron irradiation sources; (c) lunar dust pretreatment and dispersion system; (d) *in-situ* analysis system.

2.2 Cryogenic System

The cryogenic system is designed to meet the liquid nitrogen (LN_2) and gaseous nitrogen (GN_2) demands for the comprehensive environmental simulation tests within the lunar dust chamber. It consists of a liquid nitrogen storage and vaporization system, a liquid nitrogen circulation system, a gaseous nitrogen system, a cryogenic pipeline network, and a corresponding valve control system. To accommodate the high thermal load requirements under different experimental conditions, the liquid nitrogen circulation system adopts a single-phase closed-loop design.

During operation, the system first pre-cools the pipelines and thermal sinks thoroughly before filling them with liquid nitrogen. Once filled, a variable-frequency liquid nitrogen pump is activated to circulate subcooled liquid nitrogen within the thermal sinks under controlled pressure. This circulation absorbs heat from the thermal sinks, ensuring that their temperature remains stable below 100 K. The heated liquid nitrogen returns to the subcooler, where it exchanges heat with atmospheric-pressure liquid nitrogen to regain its subcooled state.

The system is equipped with a variable-frequency liquid nitrogen pump and a sub-cooler with a thermal load capacity of up to 150 kW. This configuration ensures stable operation under maximum thermal load conditions while maintaining energy efficiency during low-load operations. Additionally, optimized valve configurations enable precise control and centralized management of liquid nitrogen flow in each thermal sink branch. This design effectively mitigates potential risks to cryogenic pipelines under extreme irradiation conditions.

2.3 Lunar Dust Charging System

The lunar dust charging system (Figure 3b) is currently the only system worldwide capable of dynamically charging lunar dust particles with both positive and negative charges. It is designed to simulate the charging and discharging mechanisms of micron- and submicron-sized lunar dust under UV, X-ray, and electron irradiation, while also examining the resulting environmental effects. The system consists of a UV irradiation source, an X-ray source, an electron accelerator, and a centralized dust charging control module. The irradiation sources are evenly distributed at the upper section of the cylindrical chamber and can form a focused irradiation area with a diameter of up to 1 000 mm within the experimental zone.

The UV irradiation source consists of an array of 74 deuterium lamps, each with a power of 150 W and a wavelength range of 100–200 nm. The intensity on the irradiation surface reaches 3.5 times the standard vacuum ultraviolet (VUV) constant. To achieve large-area uniform irradiation, the source configuration employs a direct stacking method, requiring high stability, precise alignment, and accurate arrangement of the deuterium lamp array. To ensure high-intensity VUV irradiation over a meter-scale aperture, the system has optimized parameters such as the layout of the UV source interfaces, the positioning and emission angles of the deuterium lamps, and the energy distribution. Based on these calculations, a

large-aperture optical configuration and a traceability system for the deuterium lamp array have been established.

The X-ray source system provides an irradiation energy range of 30 to 80 keV. It consists of an X-ray tube assembly, a high-voltage generator, a measurement system, and a control system. X-ray irradiation induces positive surface charges of lunar dust simulants via photoelectron emission. The system features six X-ray tubes symmetrically arranged in a windmill configuration. Each tube is equipped with a dual beryllium window structure, effectively mitigating heat buildup caused by dust deposition on the vacuum windows.

The electron beam source is designed to charge dust particles via electron irradiation. It comprises a 20 keV electron gun, a high-voltage electron accelerator with an energy of 180 keV, and a 200 keV high-voltage DC power supply. The system supports both direct and deflected beam modes, enabling electron irradiation during dust sieving, dust deposition, and on the sample stage surface. The custom-designed low-energy, high-current electron gun allows adjustable beam energy between 30 and 150 keV, a current range of 1 to 15 mA, and a maximum beam power of 3.5 kW. The electron gun utilizes a thermionic emission Pierce-type design to optimize the laminar flow of the electron beam. Additionally, a solenoid coil is used to control the beam's envelope, ensuring efficient long-distance transmission of the electron beam while minimizing energy losses during the process. The system achieves a beam scanning area of 1 m × 1 m on the irradiation plane located approximately 3.5 m from the accelerator's exit. The scanning frequency is maintained at no less than 200 Hz.

2.4 Lunar Dust Pretreatment and Dispersion System

The lunar dust pretreatment and dispersion system (Figure 3c) is designed to simulate the pre-processing and uniform dispersion of lunar dust. It consists of core components such as a mechanical support frame, a dust-dispersing vehicle, a vibrating sieve device, and a dust collection opening/closing mechanism. The dust-dispersing vehicle integrates infrared heating and ultraviolet irradiation for pre-treatment, effectively removing moisture and organic contaminants from dust particles. The processed dust is then evenly spread within the dust box.

The key innovation of the system lies in the use of a vibrating sieve structure designed for large-area, high-uniformity dust dispersion. The system features interchangeable sieves to accommodate varying experimental conditions regarding dispersion area and particle size. The system also incorporates a vertically vibrating flexible sieve and a composite structure with an aluminum honeycomb panel, overcoming technical challenges related to the limited dispersion area and uniformity for micro- and nano-scale dust particles ranging from 0.1 to 100 μm. Compared to the LDAB and the LETS, the lunar dust chamber demonstrates international leadership in both dust dispersion uniformity and deposition area, with a high uniformity of over 70% across a 1 m × 1 m area. It achieves stable coefficient of variation (CV) values ranging from 0.193 to 0.221 across multiple cycles, although the uniformity is slightly lower than that of LDAB (CV < 0.11 for a 5-cm-diameter area) (Gerdts et al., 2022).

2.5 *In-situ* Analysis System

The *in-situ* analysis system (Figure 3d) serves as a critical observation platform for simulating the lunar dust environment. It is designed to monitor and record the charging characteristics, movement trajectories, and changes in the physical and chemical properties of dust particles on deposited sample surfaces in real-time during deposition and charging processes.

The system features a multi-degree-of-freedom linear motion mechanism that allows precise positioning within a 400 mm × 400 mm range on the horizontal plane of the sample stage center. The vertical movement range over the sample stage is from 0 to 60 mm, with a motion speed of no less than 400 mm/min and a positioning accuracy error controlled within ±5 mm.

The system is equipped with robust instrumentation integration capabilities, supporting the simultaneous operation of multiple analytical devices. These include high-resolution optical microscope probes, integrating sphere reflectance meters, surface emissivity meters, and electrostatic voltmeters. This provides a reliable experimental platform for the comprehensive characterization of lunar dust properties.

Based on the development trends and research progress of ground-based environmental simulation technologies for lunar exploration, three key technical challenges are currently overcome.

(1) Dynamic dust zonal charging with positive and negative charges

The dust particles on the lunar surface develop varying distributions of positive and negative charges under different irradiation sources. To simulate this complex environment, it is necessary to overcome the challenges of dust charging under multi-source irradiation. The lunar dust chamber employs a high-voltage multi-source irradiation method based on UV, X-ray, and electron beams. The chamber successfully achieves dynamic zonal control of positive and negative dust charges by establishing a physical model of dust charging and optimizing the configuration and spatial layout of irradiation sources.

This technology has realized the simulation of a lunar multi-source coupled charging environment for the first time internationally (Figure 4a). The test platform is equipped with a cold plate at the bottom, which is cooled by liquid nitrogen due to the high irradiation energy. The bright white spots in the image indicate M8 bolt markers, primarily caused by electron discharge. The blue regions represent visible light emitted from the UV lamp. Polytetrafluoroethylene (PTFE), which serves as a protective high-temperature tape in the experiments, emits a green coloration during discharge. The red regions indicate zinc oxide, serving as a fluorescent target for electron irradiation. The experiment reveals discharge phenomena oc-

curring during the dispersion process of lunar dust simulants. The UV irradiation intensity exceeds 3.5 times the standard vacuum ultraviolet constant, the X-ray source voltage reaches 80 kV, and the electron source energy reaches 150 keV. The uneven sheath electric field within the lunar dust simulants, induced by electron irradiation, induces both dust aggregation and sputtering (Cabra et al., 2025; Pagán Muñoz et al., 2024). Simultaneously, variations in the bulk density, mineral composition, specific surface area, and particle size of lunar dust simulants further intensify this migration, ultimately contributing to the formation of a dendritic distribution pattern (Figure 4b). The lunar dust chamber generates low-potential positive charges on dust through UV irradiation, high-potential positive charges through X-ray irradiation, and negative charges through electron irradiation. These three irradiation sources can operate collaboratively to accurately replicate the extreme environmental characteristics of multi-source irradiation on the lunar surface.

(2) Large-area dynamic and uniform dispersion of micron-scale dust

During lunar exploration activities, the combination of lunar microgravity and the electrostatic properties of lunar dust results in persistent dust levitation, causing dust particles to easily adhere to spacecraft surfaces and severely hinder normal exploration operations. The technical challenge faced by existing international dispersion systems is to achieve a large-area uniform distribution of micron-scale dust. The lunar dust chamber has developed an innovative composite vibrating sieve structure to overcome it. This structure integrates a vertically vibrating flexible mesh with an aluminum honeycomb panel, based on a dust particle group excitation-coupled dynamics model. The technology employs a dual-layer excitation mechanism, with coordinated operation between a vibrating dust box and a vibrating sieve, enabling dynamic uniform dispersion of dust particles ranging from 0.1 to 100 μm in size across a 1 000 mm × 1 000 mm experimental area (Figure 5a). The dispersion uniformity exceeds 70%, achieving internationally advanced technical standards (Figure 5b). This breakthrough provides a reliable technical foundation for accurately simulating the lunar dust levitation.

(3) Achieving and maintaining high-vacuum conditions under large dust-loading conditions

The accurate simulation of large-scale lunar dust environments requires ground-based equipment capable of reproducing extensive dust coverage while maintaining high vacuum conditions. The core technology involves the coordinated optimization of high-pumping speed vacuum acquisition and high vacuum maintenance. To address this challenge, the pressure differential model informs dust levitation suppression by quantifying gas flow resistance inside and outside porous lunar dust simulant piles, enabling optimized pumping speed control that prevents particle mobilization while achieving high vacuum. Controlled pumping protocols, including PID control of valve adjustments and implementation of pressure-holding phases, along with a vacuum pumping layout at the top of the chamber, balance rapid vacuum attainment

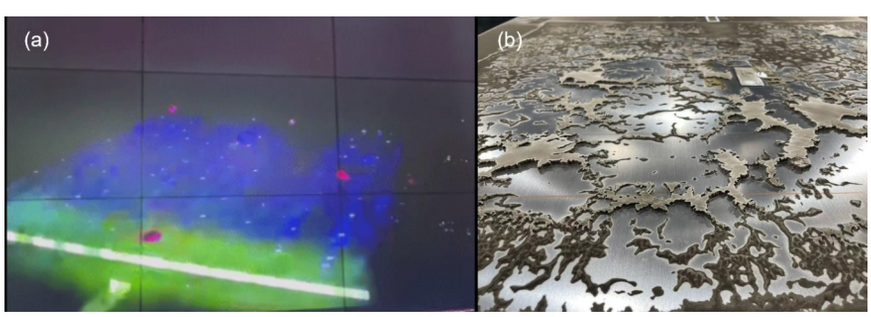

Figure 4. Dust charging and migration testing under multi-source irradiation. (a) The world's first experiment on electron-UV-X-ray coupled charging and discharging effects; (b) dust aggregation and sputtering under electron irradiation.

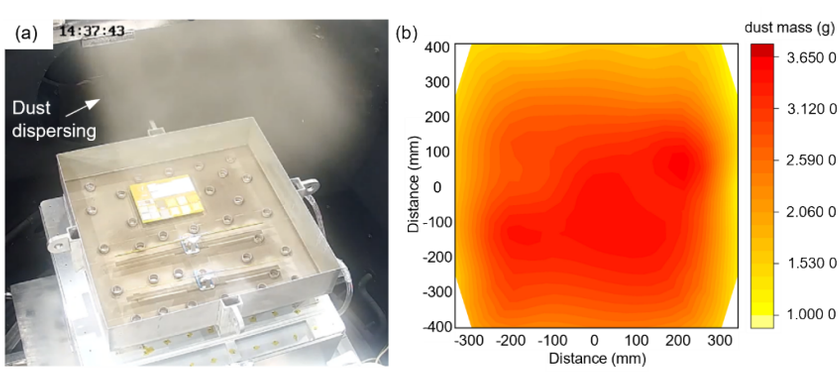

Figure 5. Large-area uniform dispersion test of micron-scale dust. (a) In-chamber monitoring of the dispersion process; (b) measured results of dispersion uniformity.

with gradual gas desorption from dust piles by minimizing turbulent gas-dust interactions. The chamber effectively mimics the lunar surface dust coverage with the integration of dust-gas permeability principles with adaptive pumping regulation.

The system adopts a multi-stage parallel vacuum acquisition design, combining a roughing system with a high-vacuum pump unit. Under conditions of a large 95 m^3 chamber volume and 30 kg of dispersed dust, the lunar dust chamber achieves an ultimate vacuum pressure of approximately 10^{-6} Pa. This performance metric is internationally advanced and provides critical technical support for high-fidelity simulation of the lunar dust environment.

3 DEVELOPMENT TRENDS IN SIMULATION TECHNOLOGY FOR LUNAR MULTI-FACTOR EXTREME ENVIRONMENT

3.1 Achieving Large-Scale, High-Fidelity Lunar Surface Simulation Environments

To support integrated testing of spacecraft components, the development of lunar environment simulation facilities requires overcoming several key technical bottlenecks, particularly in the coordinated simulation of multiple environmental factors. These include the accurate reproduction of extremely low temperatures, ultra-high vacuum, and the electrostatic properties of lunar dust. Recent advancements have significantly enhanced the capability of simulation systems to reproduce the complex lunar surface environment, providing more precise testing platforms for ground-based experimental validation. Innovative breakthroughs in precise low-temperature control, ultra-high vacuum acquisition and maintenance under large dust loads, and the simulation of dust charging characteristics under multi-source irradiation have greatly improved the realism of ground-based simulations. These advancements offer crucial experimental support and technical assurance for the development of deep-space probes and the construction of lunar bases.

3.2 Microgravity Simulation in Vacuum and Cryogenic Environments

The microgravity on the lunar surface significantly influences material behavior and physical processes, making it essential to accurately simulate this environment. Common microgravity simulation techniques include free-fall methods, airborne orbital experiments, vibration tables, and rotating platforms. These methods can provide short-term or long-term microgravity conditions and are suitable for studying the behavior of lunar dust, fluid dynamics, and material properties under microgravity. However, achieving microgravity simulation under low-temperature and vacuum conditions in limited space requires overcoming the dual challenges of extreme temperature and vacuum. Magnetic levitation platforms have demonstrated significant advantages in this regard. To ensure the reliability of experimental data, high-precision microgravity measurement technology is essential. By integrating advanced testing methods such as accelerometers, multi-channel sensor arrays, and laser interferometry systems, precise monitoring and data acquisition of material behavior in microgravity can be achieved. The combination of microgravity simulation and measurement technologies in a low-temperature vacuum environment provides a crucial experimental platform for investigating lunar surface physical phenomena and supporting *in-situ* resource utilization on the Moon.

3.3 Highly Precise *in-situ* Measurement Technology for Scalable Missions

With the continued advancement of manned lunar exploration missions, the development of lunar environment simulation equipment is moving towards higher precision, longer operational duration, and more complex environmental simulations. This trend imposes greater demands on the precise control of environmental factors and customized *in-situ* measurement capabilities. Next-generation simulation equipment must not only meet the requirements for spacecraft system-level testing but also address the diverse challenges of manned lunar exploration. These include verifying life support systems and evaluating the impact of lunar dust on both human health and equipment across various scenarios, requiring scalable and adaptable environmental simulations. Future technological development will focus on achieving breakthroughs in high-fidelity simulation, long-term stable operation, and modular system integration. These advancements will enable *in-situ* measurements for scalable missions, thereby fulfilling the complex needs of manned exploration tasks.

4 CONCLUSION

This paper reviews the fundamental characteristics of the lunar surface space environment and its key simulation factors. It provides a detailed analysis of the technical parameters, system features, and application fields of international multi-factor lunar environment simulation facilities. The paper introduces the multi-factor lunar environment simulation system, the lunar dust chamber, developed by Harbin Institute of Technology, and highlights the key technological breakthroughs achieved during its development. Building on the current state of technological advancement, the paper also proposes future development trends for large-scale lunar simulation facilities, offering valuable insights for the reliability verification of major lunar exploration missions. The lunar dust chamber will be further utilized to conduct controlled experiments on dust-plasma interactions under multi-source irradiation, the friction and wear effects of lunar dust on spacecraft functional surfaces, and dust transport under low-gravity analogs. Additionally, the chamber will focus on dust pollution from lunar exploration activities, such as manned lunar missions, long-term lunar habitation, and *in-situ* resource utilization. It will evaluate key technologies for dust prevention, control, and removal, ultimately supporting lunar and deep space exploration missions.

ACKNOWLEDGMENTS

This study was supported by the National Major Scientific and Technological Infrastructure Project "Space Environment Simulation and Research Infrastructure". This work was financially supported in part by the National Natural Science Foundation of China (No. 52275241) and the Fund for National Key Laboratory of Space Environment and Matter Behaviors (No. 2023059). The final publication is available at Springer via https://doi. org/10.1007/s12583-025-0196-3.

Conflict of Interest

The authors declare that they have no conflict of interest.

REFERENCES CITED

Cabra, A., Wang, X., Horányi, M., 2025. Laboratory Study of Dust Mobilization on Airless Planetary Bodies in the Solar Wind Plasma. *The Planetary Science Journal*, 6(2): 46. https://doi.org/10.3847/psj/adb02c

Craven, P., Vaughn, J., Schneider, T., et al., 2009. MSFC Lunar Environments Test System (LETS) System Development. Third Lunar Regolith Simulant Workshop, 17 March, Huntsville. No. M09-0391. https://ntrs. nasa. gov/api/citations/20090025947/downloads/20090025947.pdf

Criswell, D. R., 1973. Horizon-Glow and the Motion of Lunar Dust. In: Grard, R. J. L., ed., Photon and Particle Interactions with Surfaces in Space: Proceedings of the 6th Eslab Symposium, September 26–29, Noordwijk. Springer, Dordrecht. 545–556

Denevi, B. W., Noble, S. K., Christoffersen, R., et al., 2023. Space Weathering at the Moon. *Reviews in Mineralogy and Geochemistry*, 89(1): 611 – 650. https://doi. org/10.2138/rmg.2023.89.14

Gaier, J. R., Siamidis, J., Larkin, E. M., 2010. Extraction of Thermal Performance Values from Samples in the Lunar Dust Adhesion Bell Jar. 25th Space Simulation Conference, October 20 – 23, 2010, Annapolis. No. NASA/TM-2010-216828. https://permanent.fdlp.gov/gpo6964/20100039312_2010043258.pdf

Gan, H., Liu, J. H., Zhang, X. P., et al., 2025. Electrostatic Transport Characteristics of Olivine Particles under Electron Irradiation in Vacuum. *The Astrophysical Journal*, 978(1): 109–119. https://doi.org/10.3847/1538-4357/ad97be

Gerdts, S., Jimenez, N., Dunlap, P. H., Jr, 2022. Lunar Simulant Deposition Technique for Dust Tolerance Studies, January 1, Ohio. No. E-20002. https://ntrs. nasa. gov/api/citations/20210024128/downloads/TM-20210024128.pdf

Hintze, P. E., Buhler, C. R., Schuerger, A. C., et al., 2010. Alteration of Five Organic Compounds by Glow Discharge Plasma and UV Light under Simulated Mars Conditions. *Icarus*, 208(2): 749 – 757. https://doi.org/10.1016/j.icarus.2010.03.015

Immer, C., Lane, J., Metzger, P., et al., 2011. Apollo Video Photogrammetry Estimation of Plume Impingement Effects. *Icarus*, 214(1): 46 – 52. https://doi. org/10.1016/j.icarus.2011.04.018

Jin, H., Li, X. Y., Wei, G. F., et al., 2024. Properties of Lunar Dust and Their Migration on the Moon. *Space*: *Science and Technology*, 4: 142. https://doi.org/10.34133/space.0142

Mateo-Marti, E., 2014. Planetary Atmosphere and Surfaces Chamber (PASC): A Platform to Address Various Challenges in Astrobiology. *Challenges*, 5(2): 213–223. https://doi.org/10.3390/challe5020213

Morris, A. B., Goldstein, D. B., Varghese, P. L., et al., 2011. Plume Impingement on a Dusty Lunar Surface. 27th International Symposium on Rarefied Gas Dynamics, Pacific Grove, California. 1333(1): 1187 – 1192. https://doi. org/10.1063/1.3562805

Pagán Muñoz, J. H., Wang, X., Horányi, M., et al., 2024. Charging and Mobilization of Dust Particles on a Surface in Plasma. *Physical Review Letters*, 133(11): 115301. https://doi. org/10.1103/physrevlett.133.115301

Roman, K., Lavoie, J., Murzionak, P., et al., 2017. DTVAC Dusty Planetary Thermo-VACuum Simulator. 47th International Conference on Environmental Systems, July 16 – 20, 2017, Charleston. ICES-2017-235. https://ttu-ir. tdl. org/server/api/core/bitstreams/1e34b8fb-f8dd-4fa7-b031-d489d0387d2f/content

Smith, M., Craig, D., Herrmann, N., et al., 2020. The Artemis Program: An Overview of NASA's Activities to Return Humans to the Moon. 2020 IEEE Aerospace Conference. March 7 – 14, 2020, Montana. 1 – 10. https://doi. org/10.1109/aero47225.2020.9172323

Sorokin, E. G., Yakovlev, O. I., Slyuta, E. N., et al., 2020. Experimental Modeling of a Micrometeorite Impact on the Moon. *Geochemistry International*, 58(2): 113 – 127. https://doi. org/10.1134/S0016702920020111

Stubbs, T. J., Farrell, W. M., Halekas, J. S., et al., 2014. Dependence of Lunar Surface Charging on Solar Wind Plasma Conditions and Solar Irradiation. *Planetary and Space Science*, 90: 10–27. https://doi.org/10.1016/j.pss.2013.07.008

Wang, H., Phillips III, J. R., Dove, A. R., et al., 2022. Investigating Particle-Particle Electrostatic Effects on Charged Lunar Dust Transport via Discrete Element Modeling. *Advances in Space Research*, 70(10): 3231 – 3248. https://doi. org/10.1016/j.asr.2022.08.080

Wang, J. W., Gong, J., Xu, M. L., et al., 2024. Research and Development Analysis of Lunar Environment Simulation Facility. *Vacuum*, 61(5): 51 – 56. https://doi. org/10.13385/j. cnki. vacuum.2024.05.07 (in Chinese with English Abstract)

Wei, X., 2022. Research on Lunar Multi-Source Irradiation Charging Environment Simulation Technology: [Dissertation]. Harbin Institute of Technology, Harbin (in Chinese with English Abstract)

Woerner, J., Foing, B., 2016. The "Moon Village" Concept and Initiative. In: LPI Editorial Board, eds., Annual Meeting of the Lunar Exploration Analysis Group, November 1 – 3, 2016, Columbia. 1960: 5084. https://www. hou. usra. edu/meetings/leag2016/pdf/5084.pdf

Zhang, H. Y., Li, S. X., Wang, Y., et al., 2024. Nozzle plume erosion property on lunar dust in Chang'E-5 mission. *Journal of Beijing University of Aeronautics and Astronautics*, 50(4): 1251 – 1261. https://doi. org/10.13700/j. bh. 1001-5965.2022.0447 (in Chinese with English Abstract)

Zhou, C., Yu, Y., Gao, Y. Y., et al., 2024. Analysis and Implications of ESA's Moon Village Construction Program. *Journal of Civil Engineering and Management*, 41(2): 1 – 9. https://doi. org/10.13579/j. cnki. 2095-0985.2024.20230544 (in Chinese with English Abstract)